Differences in xylem and leaf hydraulic traits explain differences in drought tolerance among mature Amazon rainforest trees

DR. THOMAS POWELL (Orcid ID : 0000-0002-3516-7164)

Article type : Primary Research Articles

Title: Differences in xylem and leaf hydraulic traits explain differences in drought tolerance among mature Amazon rainforest trees

Running head: Hydraulic traits of Amazon forest trees

Authors:
Thomas L. Powell[1,2], James K. Wheeler[1,3], Alex A. R. de Oliveira[4], Antonio Carlos Lola da Costa[5], Scott R. Saleska[6], Patrick Meir[7, 8], and Paul R. Moorcroft[1*]

Affiliations:
1. Department of Organismic and Evolutionary Biology, Harvard University, Cambridge, Massachusetts, USA
2. Earth and Environmental Sciences Area, Lawrence Berkeley National Lab, Berkeley, California, USA
3. Department of Ecology and Evolutionary Biology, University of California Santa Cruz, Santa Cruz, California, USA
4. Museu Paraense Emílio Goeldi, Programa de Pós-Graduação em Biodiversidade e Evolução, Belém, Pará, Brazil
5. Centro de Geociências, Universidade Federal do Pará, Belém, Pará, Brazil
6. Department of Ecology and Evolutionary Biology, University of Arizona, Tucson, Arizona, USA
7. Research School of Biology, Australian National University, Canberra, Australia
8. School of GeoSciences, University of Edinburgh, Edinburgh, United Kingdom

*corresponding author: paul_moorcroft@harvard.edu,
ph: +1-617-496-6744

Paper type: Primary Research Article

This article has been accepted for publication and undergone full peer review but has not been through the copyediting, typesetting, pagination and proofreading process, which may lead to differences between this version and the Version of Record. Please cite this article as doi: 10.1111/gcb.13731

Abstract

Considerable uncertainty surrounds the impacts of anthropogenic climate change on the composition and structure Amazon forests. Two large-scale ecosystem drought experiments in the eastern Brazilian Amazon observed increases in mortality rates among some tree species but not others; and therefore, the physiological traits underpinning these differential demographic responses were investigated. Xylem pressure at 50% conductivity (xylem-P_{50}), leaf turgor loss point (*TLP*), cellular osmotic potential (π_o) and cellular bulk modulus of elasticity (ε), all traits mechanistically linked to drought tolerance, were measured on upper canopy branches and leaves of mature trees from selected species growing at the two drought experiment sites. Each species was placed *a priori* into one of four plant functional type (PFT) categories: drought-tolerant versus -intolerant based on observed mortality rates, subdivided into early- versus late-successional based on wood density. We tested the hypotheses that the measured traits would be significantly different between the four PFTs, and that they would be spatially-conserved across the two experimental sites. Xylem-P_{50}, *TLP*, and π_o, but not ε, occurred at significantly higher water potentials for the drought-intolerant PFT compared to the tolerant PFT; however, there were no significant differences between the early- and late-successional PFTs. These results suggest that these three traits are important for determining drought tolerance, and are largely independent of wood density—a trait commonly associated with successional status. Differences in these physiological traits that occurred between the drought-tolerant and -intolerant PFTs were conserved between the two research sites, even though they had different soil types and dry season lengths. This more detailed understanding of how xylem and leaf hydraulic traits vary between drought-tolerant and -intolerant tropical tree species that are in direct competition with each other promises to facilitate a much-needed improvement in the representation of plant

hydraulics within terrestrial biosphere models, which will enhance our ability to make robust predictions of how future changes in climate will affect tropical forests.

Key Words: Amazon rainforest, plant traits, plant hydraulics, drought, turgor loss point

Introduction

Climate model predictions indicate that dry seasons are likely to lengthen across much of the Amazon basin, with considerable overall drying in the eastern region by the end of this century (Malhi *et al.*, 2008; Joetzjer *et al*., 2013; Boisier *et al*., 2015). Widespread deforestation is also predicted to cause lower precipitation through an extensive central corridor of the basin (Coe *et al*., 2013). How these predicted changes in precipitation will affect the Amazon rainforest is, however, highly uncertain. Dynamic vegetation models are the major tool for assessing the consequences of chronic droughts; but presently, they are poorly formulated to represent contrasting physiological responses of different tree species to water stress (Gailbraith *et al*., 2010; Sakaguchi *et al*., 2011; Powell *et al*., 2013). Resolving this problem requires more detailed understanding of the mechanisms that cause mature trees to succumb to drought, and the time scale over which these mechanisms induce mortality in different species (McDowell *et al*., 2008; Hartman, 2011; McDowell *et al*., 2013, Meir *et al*., 2015a).

Two in-situ ecosystem scale drought experiments were established in the eastern Brazilian Amazon, at the Tapajós (TNF) and Caxiuanã (CAX) National Forests, to directly assess the ecological impact of a chronic 50% reduction in precipitation (Nepstad *et al*., 2007; da Costa *et al*., 2010). Two key and consistent findings emerged from both experiments: first, mortality rates of the largest trees increased by 3.0 to 4.5-fold in the drought plots, resulting in a 20% reduction in aboveground biomass after three years of drought (Nepstad *et al*., 2007; da

Costa *et al*., 2010); second, mortality rates only increased in certain species (da Costa *et al*., 2010; Rowland *et al*., 2015a). These patterns also appear to be more general across Amazonia during severe natural droughts (Phillips *et al*., 2010; Meir *et al*., 2015b). The mechanistic cause (or causes) for the differential mortality rates between species, however, has not been isolated, but plant hydraulic traits are thought to have played a key role, likely signaling a cascade of processes leading to death (Rowland *et al*., 2015b, Binks *et al*., 2016a). The similarity in mortality results amongst taxa from the two drought experiments (Nepstad *et al*., 2007, da Costa *et al*., 2010) have since made it possible to test for differences in key plant traits linked to drought sensitivity in different species.

Maintaining connectivity of water through the soil-plant-atmosphere continuum is essential for vascular plants to maintain photosynthesis. Plants manage the risk of cavitation both anatomically and through stomatal regulation of transpiration. Anatomically, wider xylem elements, larger pit membrane pores, and a higher number density of pit membranes between vessel elements can increase the efficiency of water transport and hence carbon gain, but also increase the vulnerability for embolisms to form in the xylem as tension builds (Wheeler *et al*., 2005, Choat *et al*., 2008; Poorter *et al*., 2010). The xylem pressure when 50% of conductivity is lost (xylem -P_{50}) is a useful quantitative metric for directly comparing the relative vulnerabilities of different species to cavitation during episodes of drought. Higher xylem-P_{50} values have been associated with trees growing in wetter climates in the tropics (Choat *et al*., 2007) and in larger-sized drought-intolerant tree species compared to smaller-sized trees and drought tolerant species growing at CAX (Rowland et al., 2015b). However, it is unclear if this pattern is conserved across ecosystems with contrasting soils types or if it is coordinated with other plant traits.

Plants also minimize the risk of cavitation through stomatal closure. Turgor loss point (*TLP*), the point when the leaf becomes so dehydrated its cells lose turgor, is an easily measured second order trait that correlates with the leaf water potential (ψ_{lf}) when the stomata are 50% closed (Brodribb *et al*., 2003). *TLP* has been used as an indicator of drought tolerance to low soil moisture (e.g. Lenz *et al*., 2006; Blackman *et al*., 2006). Cellular osmotic potential at full hydration (π_o) and the bulk modulus of elasticity of leaf cell walls (ε) are two first order traits that contribute to *TLP*. π_o is the amount ψ_{lf} is lowered by solutes in the cells. ε is inversely related to the volumetric change in the leaf cell as turgor declines and thus is a metric of the amount of water available from cellular storage between full hydration and *TLP*. Species with lower *TLP* and π_o are found to be more prominent in the drier climates across the tropics (Choat *et al*., 2007; Baltzer *et al*., 2008) and between dry versus wet biomes (Bartlett *et al*., 2012), as well as ecosystems with soils having comparatively lower water retention capacity (Maréchaux *et al*., 2015). Conclusive patterns for ε are more variable between these same studies (e.g Baltzer *et al*., 2008 versus Bartlett *et al*., 2012), which likely arises from other ecological reasons to have stiff leaves that correlate with drought tolerance, such as herbivory. The role of *TLP* during acute or prolonged droughts and the mechanism through which it is achieved—i.e. investment in solutes (π_o) versus cellular structure (ε) (Bartlett *et al*., 2012)—is unclear in determining mortality risk of mature tropical trees growing in competition in the same ecosystem. Furthermore, understanding the physiological determinants of *TLP* may have important implications for modeling leaf carbon-dynamics during drought, where observations indicate water-stress elevates leaf respiration; although the mechanism explaining the respiration increase has yet to be identified (Metcalfe *et al*., 2010; Rowland *et al*., 2015a).

Phenotypic plasticity of hydraulic traits of tropical species has been poorly studied in general; however, a few studies have indicated that it may be ecologically important for some species to quickly adjust to acute droughts or survive dry seasons (e.g. Fonti *et al*., 2010; Maréchaux *et al*., 2017), while others have indicated a minor role for canopy trees (Bartlett *et al*., 2014; Binks *et al*., 2016a,b, Maréchaux *et al*., 2016, 2017). Interestingly, Campanello *et al*., (2008) showed xylem conductivity of saplings increased quickly in early-successional tropical species, but remained the same in late-successional species in response to higher light levels in the understory after a simulated disturbance (Campanello *et al*., 2008). This result suggests a need to test for potential interactions between traits that select for drought tolerance and successional status. Also, another study at CAX (Binks *et al*., 2016a) found evidence for adjustment in foliar osmotic parameters to long-term (>10 yrs) experimental drought, with drought-intolerant species showing greater long-term adjustment than drought-tolerant ones.

It has been proposed that wood density may be a useful proxy for drought tolerance in tropical tree species (Fearnside, 1997), and that it is negatively correlated with the precipitation gradient that exists across the Amazon basin (Baker *et al*., 2004; but see also ter Steege *et al*., 2006). Moreover, in a pan-tropical synthesis of moist tropical forest species, a weak but significant negative relationship between π_o and wood density was found (Christoffersen *et al*., 2016). Other observational studies have found that variation in stem economic traits, such as wood density, is largely independent of hydraulic traits (Baraloto *et al*., 2010; Maréchaux *et al*., 2015). Wood density also correlates with successional type, where species with lower wood density tend to be early-successional, and species with higher wood density tend to be late-successional (Poorter *et al*., 2010). However, it has not been determined for mature trees

growing in competition within an ecosystem if the traits that define successional type co-vary or are unrelated to traits that confer drought tolerance.

In this study, we tested four hypotheses regarding the physiological underpinnings of drought tolerance at the Tapajós and Caxiuanã National Forests. The first two hypotheses concern how *TLP*, π_o, ε and xylem-P_{50} vary across species with respect to their drought-tolerance and successional status. *TLP*, π_o, and xylem-P_{50} were predicted to be more negative, and ε more positive, in canopy-sized trees that are characterized as drought-tolerant relative to intolerant (H1), and late- relative to early-successional (H2). The second two hypotheses concern spatial and temporal variation in the hydraulic traits. When variation in a hydraulic trait occurs between PFTs, the magnitude of the variation was predicted to be conserved geographically (H3) due to the similarity in observed mortality rates between the two drought experiments. Temporally, trees characterized as both drought-tolerant and early-successional were predicted to have greater plasticity in *TLP*, π_o, ε and xylem-P_{50} compared those characterized as either drought-intolerant or late-successional (H4). The examination presented here now combines drought tolerance, successional status, and multiple sites (CAX and TNF) to consider how traits controlling the hydraulic safety of canopy-dominant, seed-producing trees in the Amazon rainforest are likely to become increasingly important ecological filters if precipitation patterns change in the future.

Materials and Methods

Study Sites

The study was conducted in the two Amazon rainforest throughfall exclusion experiments (TFE) located in the Caxiuanã (CAX; 1.737ºS, 51.458ºW) and Tapajós (TNF; 2.897ºS, 54.952ºW) National Forests, Pará, Brazil. The TFEs were established to directly measure whole ecosystem

responses to severe and chronic drought (Nepstad *et al*., 2002, 2007; Brando *et al*., 2008; da Costa *et al*., 2010). The Caxiuanã TFE experiment commenced in January 2002 and was still running at the time of this study. The Tapajós TFE experiment ran from 2000 to 2004 (Nepstad *et al*., 2007); therefore *post hoc* measurements were made on the four selected species in the forest adjacent to the former TFE plots, and within-species phenotypic plasticity was not evaluated. Physical and biological characteristics of each site are summarized in Table 1.

A brief description of the TFE experimental design is given here; more detailed descriptions are provided in Nepstad *et al*. (2002) and Fisher *et al*. (2007). Two 1-ha plots, one control and one treatment plot, were established in each of the CAX and TNF forests. Both plots in each forest were selected to be structurally and floristically similar. A 1-2 m high leaky system of plastic panels and gutters was constructed over the entire understory of the treatment plot. The panels prevented approximately 50% of the rainfall from reaching the soil (Nepstad *et al*., 2002). The remaining rainfall was diverted off site through the gutters and a 1 x 1 m drainage ditch lined with plastic. The drainage ditch encircled each plot to also prevent lateral roots from accessing soil moisture from outside the plots (Nepstad *et al*., 2002). Soil moisture measurements verified the efficacy of this design to create a soil moisture drought throughout the rooting zone in the treatment plots (Fisher *et al*., 2007; Brando *et al*., 2008).

Species selection and sampling

The species measured in this study were strategically selected as representatives of four contrasting plant functional type (PFT) categories that reflect two aspects of functional diversity: drought-tolerant versus drought–intolerant, and early-successional versus late-successional (Table 2). Drought-tolerant and drought-intolerant species were identified based on mortality

rates observed in the Caxiuanã and Tapajós drought experiments (see Table 2 of da Costa *et al*., 2010). These species were then classified as early-successional or late-successional, based on whether their wood density was relatively low (<0.6 g cm^{-3}), or high (>0.8 g cm^{-3}), respectively. The early- versus late-successional classification used here is with respect to secondary successional dynamics that occurs after gap formation in tropical forests—studies have shown that light-demanding species (i.e. early successional PFTs) tend to have lower wood densities than shade tolerant species (i.e. late successional PFTs) (Muller-Landau, 2004; King *et al*., 2006; Poorter *et al*., 2010; Wright *et al*., 2010). The species selected at each site and assigned to each functional group are summarized in Table 2.

Eschweilera coriacea was found at both research sites with a sufficient number of canopy-sized individuals to construct robust pressure-volume (p-v) and xylem vulnerability curves. There were no common species for *Protium* and *Licania* between the two research sites, thus two different species were selected for each. *Inga alba* was present at both sites, but only two canopy sized individuals were present in the drought plots at CAX in 2011. Therefore, *I. gracilifolia* was measured to supplement the *Inga alba TLP* data at CAX. No significant differences were detected between the *I. alba* and *I. gracilifolia* p-v curves (data not shown).

One or two branches approximately 3 cm in diameter, 2.5 m in length, containing several branchlets and more than 100 leaves, were harvested from each individual at a height of 14 – 25 m. All branches were located in the upper crown and in full sun during the afternoon. The branches were harvested between 6:30 and 7:30 am local time, and the canopy was generally wet from rain or condensation from the night before, thus indicating minimal transpiration had yet occurred. After harvest, the branches were wrapped in plastic and the distal end was placed in water and transported for 30 to 60 minutes to the lab. The whole branches were stored in the lab

in large plastic bags with the distal ends submerged in water until the leaves or branches could be prepared for measurements on the morning of the harvest. The exact number of trees, leaves and branches sampled from each species at each site is provided in Table S1.

A total of three measurement campaigns were carried out at each site. Each campaign was over a 2-4 week period, with at least one campaign in each of the wet and dry seasons. Seasonality in the measurements was not detected and therefore the data were pooled across seasons. Measurements for CAX were made in May 2011, November 2011, and October 2012; measurements for TNF were made in January 2011, July 2011, and October 2012. Dawn and midday leaf water potential measurements were carried out on November 18, 2011, a mostly sunny day and five days since the last rain event.

Leaf hydraulic traits

Dawn and midday leaf water potentials (ψ_{lf}) were measured in the forest immediately following the branch harvest using a PMS model 600 pressure chamber (PMS Instrument Co., Albany, OR). Pressure-volume curves were constructed for each species to estimate *TLP*, π_o and ε. The p-v curves were composites of all of the leaves sampled for each species. Only fully expanded healthy leaves, either second or third from the tip, were used. Initial rehydration of the leaves was not necessary since the leaves were often wet from rain or morning dew at the time of harvest (this was also confirmed by the initial chamber balance pressure being consistently < 0.2 MPa). Each leaf was patted dry, excised from its branch, weighed to 0.0001g and then pressurized in the pressure chamber to measure the leaf water potential. The leaves were allowed to desiccate on the bench between each set of mass and pressure measurements.

TLP, π_o and ε were estimated using a change-point detection algorithm on the composite p-v curves of each species at each site (Barr *et al*., 2013). The change-point in the p-v curves occurred at the ψ_{lf} values where the F-scores were maximized for two linear models recursively fit to the upper and lower portions of the data series in each composite p-v curve. During the recursive fitting, one data point at a time was switched from the upper curve to the lower curve, where the initial upper curve and the final lower curve each included 10 data points. Then, using only the data below the ψ_{lf} value where the change-point occurred, a linear model was fit to the relationship between $1/\psi_{lf}$ (MPa) and percent water loss of the leaf (i.e. [100 – RWC] (%),where RWC was the water content of the leaf relative to saturation and equaled 100% when ψ_{lf} was 0). *TLP* was taken as the predicted value of ψ_{lf} when the lowest measured [100 – RWC] value in the relationship between $1/\psi_{lf}$ and [100 – RWC] was applied to the linear model of the relationship. π_o was equal to the inverse of the y-intercept of the linear model of relationship between $1/\psi_{lf}$ and [100 – RWC]. The slope of the line between [1, $-\pi_o$] and [(RWC at *TLP*)/100, 0] was equal to ε. Confidence intervals (CI) of 95% were established for *TLP*, π_o and ε for each species from each site by bootstrap sampling the composite p-v curves and then running the change-point detection routine for 10000 iterations. Since the bootstrapped estimates of were not normally distributed around the mean, all CIs mark the boundaries containing 95% of the bootstrapped estimates (Fig. S1). *TLP*, π_o and ε were also estimated using the methods described on PrometheusWiki (Sack *et al*., 2011). The principle difference between the change-point detection and bootstrap method and the PrometheusWiki method is in how the error of the p-v curve parameters are determined. The PrometheuusWiki approach accounts for error arising from variation between leaves. In contrast, in addition to accounting for variation between leaves, the change-point detection and boot strap method also accounts for error arising from the

uncertainty of where *TLP* actually occurs within each p-v curve of each individual leaf. The results are qualitatively the same between the two methods (see Results and Discussion); but the change-point detection results are emphasized in this report because the error estimates are more conservative (see Supporting Information, Appendix 1 for additional details about how the error estimates differ).

Xylem vulnerability

Xylem vulnerability was measured using the air-injection method (Sperry & Saliendra, 1994). This method measures the resistance of xylem vessels to air seeding as a pressure gradient builds across pit membranes separating sap-filled and air-filled vessels. This method assumes that the vulnerability of the membrane is equivalent regardless of whether the pressure gradient is pulling or pushing air through the pores. Upper canopy branch segments, approximately 11 to 13 cm in length and 0.6 cm in diameter, were inserted in a 2.7 cm double-ended pressure chamber constructed from a stainless steel, union tee, pipe adapter for 0.5 in OD inline tubes. Rubber plugs held in place with washers were used to make a seal between the branch segments and the chamber. A small section (0.5 cm) of bark was removed from each end and the middle of the branch segment to prevent flow along the bark and enable air entry into the xylem. The distal the tip was shaved with a razor and then attached to the plumbing system using a 4 cm silicon coupling. The plumbing system consisted of a 1 l lactated ringer and Tygon® tubing filled with filtered (0.2 μm) well water. The ion content of the well water was not measured and may have been different between sites. We assumed that any effects of ions on pit membrane properties were equal across all four species. Many studies have used a weak solution of KCl to control for effects of ionized water on pit membranes (e.g. Choat *et al*., 2010), which includes shrinkage of

the gelatinous film covering the microfibrils (Lee *et al*., 2012). But, it is unclear how such shrinkage impacts membrane resistance to air seeding (Rockwell *et al*., 2014).

Flow rates were measured for 10 minutes from the proximal end of the branch segment for each measurement period. On each branch segment, the native flow rate was measured first followed by a 10 minute flushing with water under ~0.1 MPa to refill highly vulnerable vessels that may have filled with an air embolism during the harvesting and preparation process. At the beginning of the campaign, we flushed 1 to 2 branch segments of each species for 30 minutes and found that flow rates equilibrated after only a few minutes in all cases. The flow rate measured after flushing was taken as the maximum flow rate. Subsequent flow rates were measured after each incremental increase in air pressure in the pressure chamber. The stem segments were disconnected from the plumbing system, pressurized for 10 minutes and then depressurized before being reconnected to the plumbing system and resuming flow. It was found on a subset of stem segments for each species that flow rates equilibrated after approximately 15 minutes after the plumbing system was reconnected. Therefore, water was allowed to flow through the stem segments for 30 minutes prior to commencing each measurement. The pressure head was between 15 and 20 cm when water was flowing through the branch.

The relationship between xylem pressure and percent loss of conductance (PLC) relative to maximum conductance of the branch segment was characterized using a Weibull function with the point where PLC reached 50% being defined as the xylem-P_{50} (Meinzer *et al*., 2009). The error estimate for xylem-P_{50} was calculated using the maximum and minimum P_{50} values that could be established from the error on the parameter estimates of the Weibull functions. An *indicator variable* (Ott, 1993) was included with each parameter of the Weibull function to test for significant categorical differences between the xylem vulnerability curves of the PFTs.

Raw data are archived in the U.S. Department of Energy NGEE-Tropics Data Archive (Powell and Moorcroft a; Powell and Moorcroft b).

Results

For all four species measured at CAX, no significant differences were detected between the control versus drought plots in either the composite pressure-volume curves (using change-point detection) or the measured xylem vulnerability curves (Figs. S2 and S3 respectively). Accordingly, data collected from the control and drought plots at CAX were combined for each set of measurements. Because the TNF drought experiment had concluded by the time of this study, within-species phenotypic plasticity during drought was not evaluated for the hydraulic traits of the species measured at TNF.

Leaf traits

Median values are the sample statistic reported for leaf traits because the bootstrapped estimates are not normally distributed; however, the significance of our results are the same if mean values are used. While the whiskers in the boxplots of Figures 1 to 3 help to identify outliers generated during the bootstrapping simulations, they do not approximate the 95% CIs because the estimates are not normally distributed around Q1 and Q3 of the box plots. Therefore, Table 3 reports the CIs marking the boundaries containing 95% of the bootstrapped estimates of the *TLP* and π_o.

A clear pattern was apparent in how *TLP* varied across the different plant functional types (Fig. 1). Median *TLPs* of the drought-intolerant species, *Inga* and *Eschweilera*, were higher than the drought-tolerant species, *Protium* and *Licania*, (ranges: -1.64 to -1.82 MPa versus -2.52 to -2.66 MPa respectively) at both TNF and CAX (Table 3, Fig. 1). In contrast, *TLP* was not

different between the early- versus late-successional PFTs. The pattern in Figure 1 showing the differences between the drought-tolerant and -intolerant PFTs is significant at the 95% CI level for all species (Table 3).

At both sites, the median cellular osmotic potentials at full hydration (π_o) of the drought-intolerant species were significantly higher (range: -1.51 to -1.76 MPa) than the drought-tolerant species (range: -2.31 to -2.40 MPa); but no significant difference was found between the early- versus late-successional species (Table 3, Fig. 2). The pattern between the drought-tolerant and -intolerant PFTs shown in Figure 2 is significant at the 95% CI level for all species (Table 3). In contrast to *TLP* and π_o, median ε was not organized by either drought tolerance or successional status and was not significantly different between any of the species at either site (Fig. 3).

TLP and π_o values were also estimated for the four species from CAX following the protocol described on PrometheusWiki (Sack *et al*., 2011) as a point of reference for the change-point detection protocol used in this study. The magnitudes of the *TLP* and π_o estimated here are comparatively lower using the change-point detection routine, and the error estimates are comparatively larger (Table 3 versus S2); however, the results are qualitatively similar with the drought-intolerant species having significantly higher values compared to the drought-tolerant species and no consistent differentiation between successional types (Tables 3 and S2).

Dawn and midday leaf water potential (ψ_{lf}) estimates for the four CAX species are reported for both the control and drought treatment plots in Table 4. Dawn ψ_{lf} for all four species were near zero in the control plots and only *Protium* was considerably (and significantly) more negative than zero (-1.15 MPa) in the drought plot (Table 4). These near-zero ψ_{lf} values at dawn were also reflected in the p-v curves for each species (Fig. S2). The control plot *Inga* and *Licania* midday ψ_{lf} were considerably higher (-0.38 and -0.14 MPa, respectively) than

Eschweilera and *Protium* ψ_{lf} (-0.74 and -1.42 MPa, respectively). There was also a significant reduction in midday ψ_{lf} of *Eschweilera*, *Protium* and *Licania* (Table 4) growing in the drought plots.

Xylem vulnerability

With the exception of the two late-successional species (*Eschweilera* and *Licania*) at TNF, the drought-intolerant species (*Inga* and *Eschweilera*) were significantly more vulnerable to xylem cavitation under decreasing xylem pressure compared to the drought-tolerant species (*Protium* and *Licania*) (IS vs. PS, CAX: $F(3, 103)=225$, $p<0.01$ and TNF: $F(3, 83)=221$, $p<0.01$; EC vs LS, CAX:$F(3, 119)=166$, $p<0.01$) (Fig. 4). Xylem-P_{50} of the drought-intolerant species was higher (range: -1.1 ± 0.1 to -1.4 ± 0.1 MPa) than that of the drought-tolerant species (range: -1.8 ± 0.1 to -2.3 ± 0.1 MPa (Table 3). The two late-successional species at TNF were a significant exception to this pattern, where the xylem-P_{50} of the drought-tolerant species (*Licania*) was -1.6 ± 0.2 MPa compared to -2.0 ± 0.1 MPa for the drought-intolerant species (*Eschweilera*) ($F(3,99)=150$, $p<0.01$). The steeper slopes of the drought-intolerant PFTs compared to the -tolerant PFTs (except at TNF) that are visible in Figure 4 are significant (see statistics above), thus demonstrating that, compared to the drought tolerant PFTs, the drought-intolerant PFTs maximizes water use for as long as possible before abruptly exceeding a catastrophic embolism threshold.

Geographic and taxonomic conservation of traits

Although the two sites were separated by 400 km and soil properties markedly differed (CAX: 78% sand versus TNF: 60% clay, Table 1), the *TLP*, π_o, and xylem-P_{50} values were generally conserved at the genus level across the two sites for all plant functional types (Table 3), with the exception of xylem-P_{50} of *Eschweilera* and *Licania* (Figs. 1, 2 and 4). The pattern and magnitude of how the traits differed between drought-tolerant versus intolerant plant functional types were also conserved for all three traits, again with the exception of *Eschweilera* and *Licania* xylem-P_{50} at TNF: at both sites the *TLP*, π_o and xylem-P_{50} of the species belonging to the drought-intolerant plant functional type were always 0.7 to 0.9 MPa higher than the values of the species belonging to the drought-tolerant plant functional type (Table 3).

Median values of π_o from each PFT in this study were compared to a recently published (Christoffersen *et al*., 2016) relationship between wood density and π_o that includes an extensive pan-tropical collection of moist tropical forest species (Fig. 5). The species measured in this study are clearly segregated within the data cloud, where the drought-tolerant PFTs are in the lower region of the relationship and the drought-intolerant PFTs are in the upper region (Fig. 5).

Discussion

In this study, we investigated how variations in leaf hydraulic traits (*TLP*, π_0, ε) and xylem vulnerability (xylem-P_{50}) correlate with drought tolerance and successional type of mature tropical trees growing in two evergreen wet tropical forests in the eastern Brazilian Amazon that were experimentally exposed to chronic drought. The tree species selected for this study represent one of four different plant functional types (Table 2). Variation in these traits has been quantified in prior studies, including tropical forests (Choat *et al*., 2007, Baltzer *et al*., 2008;

Meinzer *et al*., 2008; Bartlett *et al*., 2012; Anderegg, 2014, Maréchaux *et al*., 2015; Christoffersen *et al*., 2016). However, this study, like Rowland *et al*. (2015b) and Binks *et al*. (2016a), explicitly links measured differences in these four hydraulic traits to variation in mortality rates under experimental drought of mature tropical tree species growing in direct competition. This study also demonstrates (a) that the link between hydraulic traits and mortality is not strongly coordinated with wood density, and (b) that these observed patterns are consistent across evergreen Amazonian ecosystems with different soil characteristics.

Our results support hypothesis one (H1) that *TLP* (Fig. 1), π_o (Fig. 2) and xylem-P_{50} (Fig. 4) are generally more negative in drought-tolerant species (Table 3). Drought-tolerant PFTs appear to be gaining lower *TLPs* through differences in π_o (Fig. 2) rather than ε (Fig. 3). Our within-ecosystem results support a more general hypothesis that π_o is the dominant control over *TLP* in tree species across biomes (Lenz *et al*., 2006; Bartlett *et al*., 2012). Gaining lower *TLP* through π_o requires active transport of solutes into the cell. The observed differences in leaf cellular solute concentrations between drought-tolerant and -intolerant tree species (Fig. 2) appears to be set during leaf development and expansion, and then largely maintained until abscission, as overall respiration rates of mature fully-expanded leaves are not significantly different between the two groups under normal precipitation (Rowland *et al*., 2015a). Interestingly, drought-intolerant species measured at CAX do, however, have increased leaf respiration rates during the dry season compared to the wet season during extended drought, noting that the reported respiration rates were normalized to 25 °C (Rowland *et al*., 2015a). Therefore, when drought leads to a reduction in stomatal conductance and evaporative cooling, and thus, higher leaf temperatures in drought-intolerant trees, any concomitant increase in leaf respiration is likely to be exacerbated by other factors (Rowland *et al*., 2015a). The apparent

lack of plasticity in π_o observed in this study (Fig. S2), except for possibly in *Inga*, excludes active solute regulation as an explanation for such additional increases in leaf respiration. However, the relative increase in leaf respiration is notable in drought-intolerant species and may be attributable to energy expenditure required to repair embolized leaf xylem vessels as a consequence of having higher xylem-P_{50} and more severe dry-season water-stress.

The second hypothesis (H2), that leaf hydraulic traits (*TLP*, π_o and ε) and xylem-P_{50} differ in a consistent manner between early and late-successional species, is not supported by this study (Table 3). Our results, therefore, do not support the suggestion of Fearnside (1997) that variation in wood density is a useful proxy for establishing a combined growth/drought-tolerance axis of variation for evergreen wet tropical forests (Figs. 1, 2 and 4). Our results also contrast a strong correlation between both π_o and xylem-P_{50} and wood density that is found in deciduous dry tropical forests, which experience much more acute soil water deficits and have half as much precipitation as CAX and TNF (Zhu and Cao, 2009; Markesteijn *et al*., 2011). More generally, our results are consistent with the view that the functional trait space for evergreen tropical trees is multi-dimensional (Laughlin, 2014). For example, an earlier study of 668 neotropical tree species found that a suite of 16 leaf and stem traits operate along two distinct axes: leaf economics and wood economics (Baraloto *et al*., 2010). Or, a study of 9 leaf and hydraulic traits sampled from 85 old world tropical tree species concluded that the species were organized along a leaf economics axis and leaf hydraulics axis (Li *et al*., 2015; see also Maréchaux *et al*., 2015). Our results taken together with these earlier studies imply that there are at least three axes of functional variation in tropical forest: leaf economics, stem economics, and plant hydraulics.

It appears that the three axes of functional variation may not be entirely independent: a recent pan-tropical synthesis of tree wood density and hydraulic traits revealed a significant, but

weak, negative relationship between wood density and π_o ($R^2 = 0.08$), and a much stronger relationship ($R^2 = 0.68$) between wood density and stem capacitance (Christoffersen *et al*., 2016). By way of comparison, when the median values from Figure 2 are included with the pan-tropical wood density and π_o data for wet tropical forests, the species classified as drought-tolerant in this study occupy the lower region of the data cloud and the species classified as drought-intolerant occupy the upper region (Fig. 5), thus suggesting that ecological differences in drought vulnerability may account for some of the unexplained variation in the wood density–π_o relationship identified by Christoffersen *et al.* (2016). Furthermore, this study illustrates how a targeted species-selection approach can complement meta-analyses, as shown by Figure 5, by controlling for the methodological and site-level differences that confound aggregated data.

Leaf economic traits reflect the plants' investment of resources into the leaf for assimilating carbon (Wright *et al*., 2004; Reich, 2014; Li *et al*., 2015, Maréchaux *et al*., 2015), and stem economic traits reflect the plants investment into structure and pathogen resistance—indeed, variation in rainforest wood density appears to be better explained by the density of fiber cells and fiber cell-wall thickness compared to vessel cross-sectional area (Poorter *et al*., 2010). Plant hydraulic traits reflect how plants balance the supply of water against atmospheric demand, while not necessarily trading photosynthetic performance for water conservation (Li *et al*., 2015). Ecologically, this multidimensional functional trait space helps to explain how tropical forests can attain such high levels of taxonomic diversity since it allows for a much wider range of resource-acquisition and stress-avoidance or tolerance strategies compared to a single fast-slow axis (Reich, 2014).

We first designated the species used in this study as drought-tolerant or -intolerant based on the combined mortality-response data from the CAX and TNF drought experiments (da Costa *et al*., 2010) prior to collecting any trait information. The CAX mortality results were subsequently verified by Rowland *et al*., (2015a) and consistent with a review (Meir et al., 2015b) that includes the Sulawesi drought experiment. The selected species were then designated as early- or late-successional based on their wood density, which has been correlated with successional type (Poorter *et al*., 2010). Consequently, in the strictest sense, the hypothesis of successional status-related differences in hydraulic traits (H2) was only tested if the species evaluated in this study adhere to the general relationship between wood density and successional type (Ewel, 1980; Muller-Landau, 2004; King *et al*., 2006; Poorter *et al*., 2010, Wright et al. 2010). Nonetheless, as discussed above, our finding that wood density is not correlated with the stem and leaf hydraulic traits measured in this study implies the existence of an additional, largely independent, trait axis within evergreen tropical forest tree species.

CAX and TNF are separated by approximately 400 km, with differing meteorological conditions, and contrasting soil types and soil and water table depths (Table 1). Surprisingly, both drought experiments had similarly large increases in mortality rates and losses in aboveground biomass after 3 years despite site differences in physical properties (Nepstad *et al*., 2007; da Costa *et al*., 2010). However, because of the similarity in ecosystem responses, we tested the hypothesis that the relative differences in the plant hydraulic traits occurring between the PFTs would be spatially conserved across the two study sites (H3). The results from this study support H3 with one exception: the difference in xylem-P_{50} between *Licania* and *Eschweilera* at CAX versus TNF (Table 3, Figs. 1, 2, 4). It should be noted that our two study sites were both *terra firme* forests in the eastern portion of the Amazon basin. At present it is

unclear if these traits are similarly conserved in seasonally inundated forests or forests along the eastern flank of the Andes where on average precipitation is higher and wood density is lower (Baker *et al*., 2004; ter Steege *et al*., 2006).

Our results did not support the fourth research hypothesis (H4) that the hydraulic traits of the early-successional and drought-tolerant PFTs have plasticity in response to chronic soil water-stress: both the p-v curves and xylem vulnerability curves of the control and drought plots at CAX almost completely overlapped for each species measured (Figs. S2, S3). Limited plasticity was also reported for leaf anatomical traits (Binks *et al*., 2016b) and leaf photosynthetic capacity (Rowland *et al*., 2015a) measured on the same species at CAX, although leaf dark respiration was found to be plastic in response to long-term drought in drought-intolerant species at CAX (Rowland *et al*., 2015a). For leaf hydraulic traits, Binks *et al.* (2016a) found a relatively small (~15%), but statistically significant, degree of acclimation to long-term drought in *TLP* and π_o in a selection of drought-intolerant species that partially overlapped with those in this study. Our results of limited acclimation to drought contrast with observations of tree species endemic to seasonally dry tropical forests, which have been observed to adjust their osmotic potential by ~50% between seasons (Zhu and Cao, 2009). The reasons for the differences regarding the presence or absence of acclimation to long-term drought in *TLP* and π_o at CAX is, at present, unclear; however it may in part be due to the different species studied: specifically, Binks *et al*. (2016a) measured multiple species from *Eschweilera*, *Protium* and *Licania* genera, as well as *Manilkara bidentata*, *Pouteria anomala*, and *Swartzia racemosa*, but did not measure any *Inga* species. The differences may also reflect differences in how *TLP* and π_o were estimated from p-v curves—this issue is discussed in more detail in Appendix S1. Nonetheless, these studies, taken together with a study in French Guiana (Maréchaux *et al*.,

2017) and a pan-tropical sampling of 59 tree species (Bartlett *et al*., 2014)—both studies of evergreen tropical forests that report limited plasticity—suggest that the hydraulic traits of evergreen tropical trees have a relatively low capacity to acclimate to both acute droughts and a drier climate. In each of the evergreen tropical forest studies presented here, the mean seasonal adjustment in *TLP* was <16% (this study, Bartlett *et al*., 2014; Binks *et al*., 2016a; Maréchaux *et al*., 2017).

The ψ_{lf} measurements were taken near the end of the 2011 dry season at CAX (Table 4); a period when the ecosystem approaches its lowest available soil moisture (da Costa *et al*., 2010). Soil moisture measurements during this period indicated significantly less available soil water in the drought plots through at least 2 m rooting depth (Rowland *et al*., 2015b). *Protium tenuifolium* (early-successional drought-tolerant) was the only species measured in the treatment plot that began the day of measurement with its leaves under water-stress (Table 4). A return of ψ_{lf} to near zero is also reflected in the first points of the p-v curves for all species (Fig. S2) (noting that leaf rehydration in the lab was not part of the measurement protocol). Rehydration from morning dew may explain the near-zero ψ_{lf} values at dawn, but this should be experimentally evaluated to determine its role in alleviating water-stress. Fisher *et al*. (2006) also measured ψ_{lf} on seven tree species growing in the CAX experimental plots (*Hirtela bicornis, Lecythis confertiflora, Licania heteromorpha, Licaria ameniaca, Manilkara bidentate, Mezilaurus mahuba, Swartzia racemose*) and concluded that all of the species measured used an isohydric strategy to protect themselves from drought—i.e. where the stomata close at a ψ_{lf} well above the xylem-P_{50} thereby maintaining a relatively large safety margin. In this study, *Eschweilera* and *Protium* in the drought plots had significant decreases in their midday ψ_{lf} (Table

4), thus creating relatively narrow safety margins between ψ_{lf} and xylem-P_{50}; implying that anisohydric strategies also occur within the ecosystem.

There is a critical need for improving the representation of plant hydraulics in dynamic vegetation models that are used to predict how tropical forests will respond to severe and chronic drought (Sakaguchi *et al*., 2011; Powell *et al*., 2013; Anderegg, 2014). Significant progress has been made recently in incorporating hydrodynamics into individual-based ecosystem (e.g. Duursma and Medlyn, 2012; Christoffersen *et al*., 2016) and terrestrial biosphere (e.g. Xu *et al*., 2016) models. However, the water-stress parameterizations in these models still lack diversity in xylem cavitation curves (e.g Fig. 4) and stomatal sensitivity to *TLP* (e.g. Fig. 1) as show by Brodribb *et al*. (2003). Prior to this study, Rowland *et al*. (2015b), and Binks *et al*., (2016a), it was not clear if the observed variation in hydraulic traits correlated with differential mortality rates during extended severe droughts, or if it was related to a separate ecological process such as successional dynamics (Campanello *et al*., 2008; Markesteijn *et al*., 2011). Therefore, the evidence from these studies argue for dynamic vegetation models to include multiple tropical tree PFTs with contrasting water-stress parameterizations when they are used to evaluate the effects of severe drought in the tropics. Moreover, the PFT specific traits measured in this study map directly onto the parameters used in hydrodynamic model formulations (e.g. SPA-Williams *et al*., 1996; FETCH-Bohrer *et al*., 2005; and ED2 with hydrodynamics-Xu *et al.*, 2016), thus enabling a mechanistically-based evaluation of the role of functional diversity in hydrodynamic traits in tropical forest ecosystems. For example, preliminary analyses using xylem-P_{50} and *TLP* values from this study to parameterize drought-tolerant and -intolerant PFTs in ED2 with hydrodynamics (Xu *et al*., 2016, a terrestrial biosphere model with size-structured dynamic vegetation,) indicate that the observed differences of 0.75 MPa for these traits are ecologically

significant for facilitating functional diversity along a drought tolerance axis of competition, but when the differences are <0.75 MPa, coexistence of both drought-tolerant and -intolerant PFTs fails to occur (Powell, 2016). This study also provides information about the uncertainty of *TLP* (Table 3, Figs. 1, S1) and xylem-P_{50} (Table 3) estimates for drought-tolerant and drought-intolerant tropical species, which is critical for constraining hydrodynamic formulations of different PFTs. While our study supports including a greater number of hydraulically defined PFTs in dynamic vegetation models, it does not provide strong support for having the hydraulic traits of each modeled PFT vary spatially (Figs. 1-4) or temporally (Figs. S2, S3).

This study has found a characteristic pattern in the measured leaf and xylem traits of several tropical tree species that is consistent with their demographic responses to experimentally-imposed drought conditions. Therefore, this study provides valuable insight into the traits controlling drought tolerance of tropical rainforest trees and provides much needed information for parameterizing more realistic water-stress functions in terrestrial biosphere models. Evidence from this study supports H1 thereby suggesting that the leaf traits, *TLP* and π_o and the stem trait, xylem-P_{50}, are associated with drought tolerance in tropical trees. This study, however, does not support H2 in that these three traits do not vary with wood density, an important life history trait associated with succession; thus supporting the hypothesis that variation in plant hydraulic traits is largely independent from both the stem and leaf economic traits axes for tropical rainforest trees. The evidence from this study also supports H3 and rejects H4, thus suggesting that hydraulic traits of *terra firme* Amazonian trees are largely conserved spatially and temporally. However, although there appears to be some species variation in the plasticity of hydraulic traits, the overall limited degree of plasticity indicates that mature trees belonging to the drought-intolerant functional type are vulnerable to reductions in precipitation

because of their limited ability to adjust. Finally, we find that variability in plant hydraulic traits does exist among tropical tree species, and this variability may have been—and will be—critical in determining the fate of the Amazon rainforest if precipitation patterns change substantially.

Acknowledgments

This research was funded by a National Science Foundation Doctoral Dissertation Improvement Grant (NSF award # DEB-1110540), the National Science Foundation Partnership for International Research and Education in Amazon Climate Interactions grant (NSF award #OISE-0730305), a grant from the Andes-Amazon Initiative of The Gordon and Betty Moore Foundation, graduate research funding from the Department of Organismic and Evolutionary Biology, Harvard University, and the Office of Biological and Environmental Research, US Department of Energy, NGEE-Tropics project. PM was supported by NERC NE/J011002/1 and ARC FT110100457. We thank the Museu Paraense Emilio Goeldi, the LBA office in Santarém, and the many dedicated field technicians who provided logistical support and assistance collecting samples. We are extremely grateful to Tony Rockwell, Missy Holbrook, and Kathy Ran for their instruction or assistance with the field measurements.

References

Anderegg WRL (2014) Spatial and temporal variation in plant hydraulic traits and their relevance for climate change impacts on vegetation. *New Phytologist*, **205**, 1008-1014. doi: 10.1111/nph.12907.

Baker TR, Phillips OL, Malhi Y, et al. (2004) Variation in wood density determines spatial patterns in Amazonian forest biomass. *Global Change Biology*, **10**, 545–562, doi: 10.1111/j.1529-8817.2003.00751.x.

Baltzer JL, Davies SJ, Bunyavejchewin S, Noor NSM (2008) The role of desiccation tolerance in determining tree species distributions along the Malay–Thai Peninsula *Functional Ecology*, **22**, 221–231 doi: 10.1111/j.1365-2435.2007.01374.x

Baraloto C, Paine CET, Poorter L, Beauchene J, Bonal D, Domenach A-M, Hérault B, Patiño S, Roggy J-C, Chave J (2010) Decoupled leaf and stem economics in rain forest trees. *Ecology Letters*, **13**, 1338-1347. doi: 10.1111/j.1461-0248.2010.01517.x.

Barr AG, Richardson AD, Hollinger DY, *et al.* (2013) Ude of change-point detection for friction-velocity threshold evaluation in eddy-covariance studies. *Agricultural and Forest Meteorology*, **171-172**, 31-45. doi: 10.1016/j.agrformet.2012.11.023.

Bartlett MK, Scoffoni C, Sack L (2012) The determinants of leaf tugor loss point and prediction of drought tolerance of species and biomes: a global meta-analysis. *Ecology Letters*, **15**, 393-405. dio: 10:1111/j.1461-0248.2012.01751.x.

Bartlett MK, Zhang Ya, Kreidler N, Sun S, Ardy R, Cao K, Sack L (2014) Global analysis of plasticity in turgor loss point, a key drought tolerance trait. *Ecology Letters*, **17**, 1580-1590. doi: 10.1111/ele.12374

Binks O, Meir P, Rowland L, da Costa ACL, Vasconcelos SS, Oliveira AAR, Ferreira L, Christoffersen B, Nardini A, Mencuccini M (2016a) Plasticity in leaf-level water relations of

tropical rainforest trees in response to experimental drought. *New Phytologist*, **211**, 477-488. doi: 10.1111/nph.13927

Binks O, Meir P, Rowland L, da Costa ACL, Vasconcelos SS, Oliveira AAR, Ferreira L, Mencuccini M (2016b) Limited acclimation in leaf anatomy to experimental drought in tropical rainforest trees. *Tree Physiology*. doi: 10.1093/treephys/tpw078.

Blackman CJ, Brodribb TJ, Jordan GJ (2010) Leaf hydraulic vulnerability is releated to conduit dimensions and drought resistance across a diverse range of woody angiosperms. *New Phytologist*, **188**, 1113–1123. doi: 10.1111/j.1469-8137.2010.03439.x

Bohrer G, Mourad H, Laursen TA, Drewry D, Avissar R, Poggi D, Oren R, Katul GG (2005) Finite element tree crown hydrodynamics model (FETCH) using porous media flow within branching elements: A new representation of tree hydrodynamics. *Water Resources Research*, **41**, W11404. doi: 10.1029/2005WR004181.

Boisier JP, Ciais P, Ducharne A, Guimberteau M (2015) Projected strengthening of Amazonian dry season by constrained climate model simulations. *Nature Climate Change*, **5**, 656-660. doi: 10.1038/nclimate2658.

Brando PM, Nepstad DC, Davidson EA, Trumbore SE, Ray D, Camargo P (2008) Drought effects on litterfall, wood production and belowground carbon cycling in an Amazon forest:

results of a throughfall reduction experiment *Philosophical Transactions of the Royal Society B*, **363**, 1839–1848. doi:10.1098/rstb.2007.0031

Brodribb TJ, Holbrook NM, Edwards EJ, Gutiérrez MV (2003) Relations between stomatal closure, leaf tugor and xylem vulnerability in eight tropical dry forest trees. *Plant, Cell and Environment*¸ **26**, 433-450.

Campanello PI, Gatti MG, Goldstein G (2008) Coordination between water-transport efficiency and photosynthetic capacity in canopy tree species at different growth irradiances. *Tree Physiology*, **28**, 85-94.

Choat B, Sack L, Holbrook NM (2007) Diversity of hydraulic traits in nine *Cordia* species growing in tropical forests with contrasting precipitation. *New Phytologist*, **175**, 686-698. doi: 10.1111/j.1469-8137.2007.02137.x

Choat B, Cobb AR, Jansen S (2008) Structure and function of bordered pits: new discoveries and impacts on whole-plant hydraulic function. *New Phytologist*, **177**, 608-626. doi: 10.1111/j.1469-8137.2007.02317.x

Choat B, Drayton WM, Brodersen C, Matthews MA, Shackel KA, Wada H, McElrone AJ (2010) Measurements of vulnerability to water stress-induced cavitation in grapevine: a comparison of four techniques applied to long-vesseled species. *Plant, Cell and Environment*, **33**, 1502-1512. doi: 10.1111/j.1365-3040.2010.02160.x

Christoffersen BO, Gloor M, Fauset S, *et al.* (2016) Linking hydraulic traits to tropical forest function in a size-structured and trait-driven model (TFS v.1-Hydro). *Geoscientific Model Development*, **9**. doi: 10.5194/gmd-9-1-2016.

Coe MT, Marthews TR, Costa MH, *et al*. (2013) Deforestation and climate feedbacks threaten the ecological integrity of south southeastern Amazonia. Phil Trans R Soc B **368**, 20120155. doi.org/10.1098/rstb.2012.0155

da Costa ACL, Galbraith D, Almeida S, *et al.* (2010) Effect of 7 yr of experimental drought on vegetation dynamics and biomass storage of an eastern Amazonian rainforest. *New Phytologist*, **187**, 579–591. doi: 10.1111/j.1469-8137.2010.03309.x

Duursma RA, Medlyn BE (2012) MAESPA: a model to study interactions between water limitation, environmental drivers and vegetation function at tree and stand levels, with an example application to [CO_2] x drought interactions. *Geoscientific Model Development*, **5**, 919-940. doi: 10.5194/gmd-5-919-2012.

Ewel J (1980) Tropical succession: manifold routes to maturity. *Biotropica*, **12**, 2-7. doi: 10.2307/2388149.

Fearnside PM (1997) Wood density for estimating forest biomass in Brazilian Amazonia. *Forest Ecology and Management*, **90**, 59-87.

Fisher RA, Williams M, Lobo do Vale, da Costa AL, Meir P (2006) Evidence from Amazonian forest is consistent with isohydric control of leaf water potential. *Plant, Cell and Environment*, **29**, 151-165.

Fisher RA, Williams M, da Costa AL, Malhi Y, da Costa RF, Almeida S, Meir P (2007) The response of an Eastern Amazonian rain forest to drought stress: results and modelling analyses from a throughfall exclusion experiment. *Global Change Biology*, **13**, 2361-2378.

Fonti P, von Arx G, García-González I, Eilmann B, Sass-Klaassen U, Gärtner H, Eckstein (2010) Studying global change through investigation of the plastic responses of xylem anatomy in tree rings. *New Phytologist*, **185**, 42-53. doi: 10.1111/j.1469-8137.2009.03030.x.

Galbraith D, Levy PE, Sitch S, Huntingford C, Cox P, Williams M, Meir P (2010) Multiple mechanisms of Amazonian forest biomass losses in three dynamic global vegetation models under climate change. *New Phytologist*, **187**, 647-665. doi: 10.1111/j.1469-8137.2010.03350.x

Hartmann H (2011) Will a 385 million year-struggle for light become a struggle for water and for carbon? – How trees may cope with more frequent climate change-type drought events. *Global Change Biology*, **17**, 642-655. doi: 10.1111/j.1365-2486.2010.02248.x

Joetzjer E, Douville H, Delire C, Ciais P (2013) Present-day and future Amazonian precipitation in global climate models: CMIP5 versus CMIP3. *Climate Dynamics*. doi: 10.1007/s00382-012-1644-1

King DA, Davies SJ, Tan S, Nur Supardi MN (2006) The role of wood density and stem support costs in the growth and mortality of tropical trees: tree demography and stem support costs. *Journal of Ecology*, **94**, 670–80. doi:10.1111/j.1365-2745.2006.01112.x.

Laughlin DC (2014) The intrinsic dimensionality of plant traits and its relevance to community assembly. *Journal of Ecology*, **102**, 186-193. doi: 10.1111/1365-2745.12187.

Lee J, Holbrook NM, Zwieniecki MA (2012) Ion induced changes in the structure of bordered pit membranes. *Frontiers in Plant Science*, **3**. doi: 10.3389/fpls.2012.00055

Lenz TI, Wright IJ, Westoby M (2006) Interrelations among pressure-volume curve traits across species and water availability gradients. *Physiologia Plantarum*, **127**, 423-433. doi: 10:1111/j.1399-3054.2006.00680.x.

Li L, McCormack ML, Ma C, Kong D, Zhang Q, Chen X, Zeng H, Niinemets U, Guo D (2015) Leaf economics and hydraulic traits are decoupled in five species-rich tropical-subtropical forests. *Ecology Letters*, **18**, 899-906. doi: 10.1111/ele.12466.

Malhi Y, Roberts JT, Betts RA, Killeen TJ, Li W, Nobre CA (2008) Climate change, deforestation, and the fate of the Amazon. *Science*, **319**, 169. doi: 10.1126/science.1146961.

Maréchaux I, Bartlett MK, Sack L, Baraloto C, Engel J, Joetzjer E, Chave J (2015) Drought tolerance as predicted by leaf water potential at turgor loss point varies strongly across species within an Amazonian forest. *Functional Ecology*, **29**, 1268-1277. doi: 10.1111/1365-2435.12452.

Maréchaux I, Bartlett MK, Gaucher P, Sack L, Chave J (2016) Causes of variation in leaf-level drought tolerance within an Amazonian forest. *Journal of Plant Hydraulics*. doi: 10.20870/jph.2016.e004.

Maréchaux I, Bartlett MK, Iribar A, Sack L, Chave J (2017) Stronger seasonal adjustment in leaf turgor loss point in lianas than trees in an Amazonian forest. *Biology Letters*, **13**. http://dx.doi.org/10.1098/rsbl.2016.0819

Markesteijn L, Poorter L, Bongers F, Paz, H, Sack L (2011) Hydrualics and life history of tropical dry forest tree species: coordination of species' drought and shade tolerance. *New Phytologist*, **191**, 480-495. doi: 10.1111/j.1469-8137.2011.03708.x

McDowell N, Pockman WT, Allen CD, *et al*. (2008) Mechansims of plant survival and mortality during drought: why do some plants survive while other succumb to drought? *New Phytologist*, **178**, 719-739. doi: 10.1111/j.1469-8137.2008.02436.x.

McDowell N, Ryan MG, Zeppel MJB, Tissue D (2013) Improving our knowledge of drought-induced forest mortality through experiments, observations, and modeling *New Phytologist*, **200**, 289-293.

Meinzer FC, Campanello PI, Domec J-C, Gatti MG, Goldstein G, Villalobos-Vega R, Woodruff DR (2008) Constraints on physiological function associated with branch architecture and wood density in tropical forest trees. *Tree Physiology*, **28**, 1609-1617.

Meinzer FC, Johnson DM, Lachenbruch B, McCulloh KA, Woodruff DR (2009) Xylem hydraulic safety margins in woody plants: coordination of stomatal control of xylem tension with hydraulic capacitance. *Functional Ecology*, **23**, 922-930. doi: 10.1111/j.1365-2435.2009.01588.x.

Meir P, Mencuccini M, Dewar RC (2015a) Drought-related tree mortality: addressing the gaps in understanding and prediction. *New Phytologist*, **207**, 28-33. doi:10.1111/nph.13382.

Meir P, Wood TE, Galbraith DR, Brando PM, da Costa ACL, Rowland L, Ferreira LV (2015b) Threshold responses to soil moisture deficit by trees and soil in tropical rain forests: insights from field experiments. *Bioscience*, **9**, 882-892.

Metcalfe DB, Lobo-do-Vale R, Chaves MM, *et al.* (2010). Impacts of experimentally imposed drought on leaf respiration and morphology in an Amazon rainforest. *Functional Ecology* **24:** 524-533. doi: 10.1111/j.1365-2435.2009.01683.x

Muller-Landau HC (2004) Interspecific and inter-site variation in wood specific gravity of tropical trees. *Biotropica*, **36**, 20–32. doi: 10.1111/j.1744-7429.2004.tb00292.x

Nepstad DC, Moutinho P, Dias-Filho MB, *et al.* (2002) The effects of partial throughfall exclusion on canopy processes, aboveground production, and biogeochemistry of an Amazon forest. *Journal of Geophysical Research* **107(D20)**, 8085. doi:10.1029/2001JD000360.

Nepstad DC, Tohver IM, Ray D, Moutinho P, Cardinot G (2007) Mortality of large trees and lianas following experimental drought in an Amazon forest. *Ecology*, **88**, 2259-2269.

Ott RL (1993) *An Introduction to Statistical Methods and Data Analysis*. Fourth Edition. Duxbury Press, Belmont, California, USA.

Phillips OL, van der Heijden G, Lewis S, *et al*. (2010) Drought-mortality relationships for tropical forests. *New Phytologist*, **187**, 631-646. doi: 10.1111/j.1469-8137.2010.03359.x

Poorter L, McDonald I, Alarcon A, *et al*. (2010) The importance of wood traits and hydraulic conductance for the performance and life history strategies of 42 rainforest tree species. *New Phytologist*, **185**, 81-492. doi: 10.1111/j.1469-8137.2009.03092.x.

Powell TL (2015) Determining drought sensitivity of Amazon forest: does plant hydraulics matter? Dissertation. Harvard University, Cambridge, Massachusetts, USA.

Powell T, Moorcroft P (a) Leaf Pressure Volume Data in Caxiuana and Tapajos National Forest, Para, Brazil (2011). NGEE Tropics Data Collection. Accessed at http://dx.doi.org/10.15486/NGT/1347606

Powell T, Moorcroft P (b) Xylem vulnerability curves of canopy branches of mature trees from Caxiuana and Tapajos National Forests, Para, Brazil. NGEE Tropics Data Collection. Accessed at http://dx.doi.org/10.15486/NGT/1347607

Powell TL, Galbraith DR, Christoffersen BO, *et al*. (2013) Confronting model predictions of carbon fluxes with measurements of Amazon forests subjected to experimental drought. *New Phytologist*, **200**, 350-364. doi: 10.1111/nph.12390

Reich PB (2014) The world-wide 'fast-slow' plant economics spectrum: a traits manifesto. *Journal of Ecology*, **102**, 275-301. doi: 10.1111/1365-2745.12211.

Rockwell FE, Wheeler JK, Holbrook NM (2014) Cavitation and its discontents: opportunities for resolving current controversies. *Plant Physiology*, **164**, 1649 – 1660. doi:10.1104/pp.113.233817

Rosolem R, Shuttleworth WJ, Gonçalves LGG (2008) Is the data collection period of the Large-Scale Biosphere-Atmosphere Experiment in Amazonia representative of long-term climatology? *Journal of Geophysical Research*, **113**, G00B09, doi:10.1029/2007JG000628.

Rowland L, Lobo-Do-Vale RL, Christoffersen BO, et al., (2015a) After more than a decade of soil moisture deficit, tropical rainforest trees maintain photosynthetic capacity, despite increased leaf respiration. *Global Change Biology*, **21**, 4662 – 4672. doi: 10.1111/gcb.13035.

Rowland L, da Costa ACL, Galbraith DR, *et al.* (2015b) Death from drought in tropical forests is triggered by hydraulics not carbon starvation. *Nature*, **528**, 119-122. doi: 10/1038/nature15539.

Ryan MG, Phillips N, Bond BJ (2006) The hydraulic limitation hypothesis revisited. *Plant, Cell and Environment*, **29**, 367-381. doi: 10.1111/j.1365-3040.2005.01478.x.

Sack L, Pasquet-Kok J, PrometheusWiki contributors (2011) "Leaf pressure-volume curve parameters," *PrometheusWiki*, http://www.publish.csiro.au/prometheuswiki/tiki-pagehistory.php?page=Leaf pressure-volume curve parameters&preview=16 (accessed February 24, 2014)

Sakaguchi K, Zeng X, Christoffersen BJ, Restrepo-Coupe N, Saleska SR, Brando PM (2011) Natural and drought scenarios in an east central Amazon forest: Fidelity of the Community Land Model 3.5 with three biogeochemical models. *Journal of Geophysical Research*, **116**: G01029. doi:10.1029/2010JG001477.

Sperry JS, Saliendra NZ (1994) Intra- and inter-plant variation in xylem cavitation in *Betula occidentalis*. *Plant, Cell and Environment*, **17**, 1233-1241.

ter Steege H, Pitman NCA, Phillips OL, *et al*. (2006) Continental-scale patterns of canopy tree composition and function across Amazonia. *Nature*, **443**, 444-447. doi:10.1038/nature05134.

ter Steege H, Pitman NCA, Sabatier D, *et al.* (2013) Hyperdominance in the Amazonian tree flora. *Science*, **342**, 1243092. doi: 10.1126/science.1243092.

Wheeler JK, Sperry JS, Hacke UG, Hoang N (2005) Inter-vessel pitting and cavitation in woody Rosaceae and other vesselled plants: a basis for a safety versus efficiency trade-off in xylem transport. *Plant, Cell and Environment*, **28**, 800-812.

Williams M, Rastetter EB, Fernandes DN, Goulden ML, Wofsy SC, Shaver GR, Melillo JM, Munger JW, Fan S-M, Nadelhoffer KJ (1996) Modelling the soil-plant-atmosphere continuum in a *Quercus-Acer* stand at Harvard Forest: the regulation of stomatal conductance by light, nitrogen and soil/plant hydraulic properties. *Plant, Cell and Environment*, **19**, 911–927.

Wright IJ, Reich PB, Westoby M, *et al*. (2004) The worldwide leaf economics spectrum. *Nature*, **428**, 821-827.

Wright SJ, Kitajima K, Kraft NJB, *et al.* (2010) Functional traits and the growth-mortality trade-off in tropical trees. *Ecology*, **91**, 3664-3674.

Xu X, Medvigy D, Powers J, Becknell J, Guan K (2016) Hydrological niche separation explains seasonal and inter-annual variations in seasonally dry tropical forests. *New Phytologist*. doi: 10.1111/nph.14009.

Zhu S-D, Cao K-F (2009) Hydraulic properties and photosynthetic rates in co-occurring lianas and trees in a seasonal tropical rainforest in southwestern China. *Plant Ecology*, **204**, 295-304. doi:10.1007/s11258-009-9592-5.

Tables and Figures Captions

Table 1. Physical and biological characteristics of the Caxiuanã and Tapajós National Forest throughfall exclusion sites.

Table 2. Species selected to represent each plant functional group. Sites are noted by CAX for Caxiuanã and TNF for Tapajós National Forests.

Table 3. Leaf and xylem trait estimates ±95% confidence intervals for each species representing one of the four plant functional types at the Caxiuanã (CAX) and Tapajós (TNF) National Forests. IS: *Inga* species. EC: *Eschweilera coriacea*. PS: *Protium* species. LS: *Licania* species. TLP: leaf tugor loss point. π_o: leaf osmotic potential. Xylem-P_{50}: water potential when 50% of conductance is lost. The leaf traits estimates are the median bootstrapped value using the change-point detection routine. Xylem-P_{50}s are based on a Weibull-curve best-fit for each species.

Table 4. Mean ±SE dawn and midday leaf water potential (ψ_{lf}, MPa) measured at Caxiuanã in the control and treatment plots on 11/18/2011. Each species represents one of the four plant functional types evaluated in this study: drought-tolerant versus -intolerant and early- versus late-successional (Table 2).

Figure 1. Distribution of turgor loss point (TLP, MPa) estimates for each plant functional type measured at the Tapajós (TNF) and Caxiuanã (CAX) National Forests. IS: *Inga* species, early-successional drought-intolerant. EC: *Eschweilera coriacea*, late-successional drought-intolerant. PS: *Protium* species, early-successional drought-tolerant. LS: *Licania* species, late-successional drought-tolerant. The boxes show the interquartile range (IQR) between 25% (Q1) and 75% (Q3) of the values, horizontal black bars are the median value, whiskers define the "fence" = [Q1, Q3] + 1.57 × IQR, the symbols are outliers beyond the fence.

Figure 2. Distribution of bulk leaf osmotic potentials (π_o, MPa) for each plant functional type measured at the Tapajós (TNF) and Caxiuanã (CAX) National Forests. IS: *Inga* species, early-

successional drought-intolerant. EC: *Eschweilera coriacea*, late-successional drought-intolerant. PS: *Protium* species, early-successional drought-tolerant. LS: *Licania* species, late-successional drought-tolerant. The boxes show the interquartile range (IQR) between 25% (Q1) and 75% (Q3) of the values, horizontal black bars are the median value, whiskers define the "fence" = [Q1, Q3] + 1.57 × IQR, the symbols are outliers beyond the fence.

Figure 3. Distribution of the bulk leaf modulus of elasticity (ε, MPa) for each plant functional type measured at the Tapajós (TNF) and Caxiuanã (CAX) National Forests. IS: *Inga* species, early-successional drought-intolerant. EC: *Eschweilera coriacea*, late-successional drought-intolerant. PS: *Protium* species, early-successional drought-tolerant. LS: *Licania* species, late-successional drought-tolerant. Note: outliers for LS at CAX extend to 186 MPa. The boxes show the interquartile range (IQR) between 25% (Q1) and 75% (Q3) of the values, horizontal black bars are the median value, whiskers define the "fence" = [Q1, Q3] + 1.57 × IQR, the symbols are outliers beyond the fence.

Figure 4. Xylem vulnerability curves showing the percent loss of conductivity (PLC) with decreasing xylem pressure (MPa) of the selected species representing the four plant functional types measured at the Tapajós (TNF, open symbols) and Caxiuanã (CAX, closed symbols) National Forests. (a) *Inga*: early-successional drought-intolerant. (b) *Eschweilera*: late-successional drought-intolerant. (c) *Protium*: early-successional drought-tolerant. (d) *Licania*: late-successional drought-tolerant. Vertical lines indicate point when 50% loss of conductance (P_{50}) was reached for the TNF (dashed) and CAX (solid) species (see Table 3 for mean±CI values).

Figure 5. Relationship between bulk leaf osmotic potential (π_o, MPa) and wood density. Open black symbols are pan-tropical values for moist tropical forests from Figure 2b of Christoffersen *et al*. (2016). The closed colored symbols are the species measured in this study representing each plant functional type (PFT) from the Caxiuanã (CAX, circles) and Tapajós (TNF, triangles) National Forests. IS: *Inga* species, early-successional drought-intolerant (green). EC: *Eschweilera coriacea*, late-successional drought-intolerant (gold). PS: *Protium* species, early-successional drought-tolerant (blue). LS: *Licania* species, late-successional drought-tolerant (red).

Table 1.

Characteristic	Caxiuanã	Tapajós	Reference
Mean annual precipitation	2272 mm	2000 mm	Fisher *et al*., 2007, Nepstad *et al*., 2002
Wet season (>100 mm mo^{-1})	Dec. to mid-Jul.	Dec. to mid-Jun.	Rosolem *et al.*, 2008
Soil type	clay: 15% sand: 78%	clay: 60% sand: 38%	Fisher *et al*., 2007, Nepstad *et al*., 2002
Water table depth	10 m	>80 m	Fisher *et al*., 2007, Nepstad *et al*., 2002
Aboveground biomass of trees >10 cm dbh	214 t C ha^{-1}	150 t C ha^{-1}	da Costa *et al.*, 2010, Nepstad *et al*., 2002

Table 2.

Drought Sensitivity	**Succession**	
	Early	**Late**
Intolerant	**Genus: *Inga*** CAX: *I. alba, I. gracilifolia* Ducke TNF: *I. alba* (SW.)Willd.	**Genus: *Eschweilera*** CAX: *E. coriacea* (DC.) S.A.Mori TNF: *E. coriacea*
Tolerant	**Genus: *Protium*** CAX: *P.tenuifolium* Engl. TNF: *P. robustum* (Swart.) Porter	**Genus: *Licania*** CAX: *L. octandra* (Kuntze) TNF: *L. canescens* R. Benoist

.

Table 3.

Drought sensitivity	Successional type (Species ID)	Trait:	TLP		π_o		Xylem-P_{50}	
		Site:	CAX	TNF	CAX	TNF	CAX	TNF
Intolerant	Early (IS)		−1.82 +0.11,−0.29	−1.70 +0.14,−0.27	−1.76 +0.11,−0.23	−1.62 +0.13,−0.23	−1.4±0.1	−1.1±0.1
	Late (EC)		−1.80 +0.42,−0.42	−1.64 +0.13,−0.13	−1.70 +0.40,−0.39	−1.51 +0.07,−0.08	−1.2±0.1	−2.0±0.1
Tolerant	Early (PS)		−2.52 +0.15,−0.40	−2.66 +0.45,−0.22	−2.35 +0.18,−0.30	−2.31 +0.34,−0.18	−2.3±0.1	−1.8±0.1
	Late (LS)		−2.56 +0.42,−0.28	−2.55 +0.42,−0.76	−2.40 +0.33,−0.19	−2.36 +0.36,−0.74	−2.2±0.2	−1.6±0.2

Table 4

Drought Tolerance	Succession	Species	Midday ψ_{lf} (MPa)		Dawn ψ_{lf} (MPa)	
			Control	Treatment	Control	Treatment
Intolerant	Early	*Inga alba*	-0.38±0.06	-0.44±0.17	-0.04±0.01	-0.03±0.01
	Late	*Eschweilera coriacea*	-0.74±0.08*	-1.95±0.13*	-0.08±0.01*	-0.04±0.01*
Tolerant	Early	*Protium tenuifolium*	-1.42±0.03*	-1.91±0.04*	-0.18±0.04*	-1.15±0.10*
	Late	*Licania octandra*	-0.14±0.02*	-0.35±0.04*	-0.07±0.01	-0.06±0.01

*Indicates significant treatment effect where $|t| > t_{\alpha/2}$, $\alpha = 0.05$.

Supporting Information

The following Supporting Information may be found in the online version of this article:

Appendix S1. Ancillary discussion of methods.

Table S1. Leaf and branch sample sizes for each species at each site. Leaves were used to construct the pressure-volume curves shown in Figure S2 and branches were used to construct the xylem vulnerability curves shown in Figure S3. Sites are indicated by CAX for Caxiuanã and TNF for Tapajós National Forests.

Table S2. Turgor loss point (TLP) and bulk leaf osmotic potential (π_o) estimates (mean ± SE) using the methods described by Sack et al. (2011) on PrometheusWiki. Trait values are given for the four species representing one of the four plant functional types characterized in this study for Caxiuanã National Forest (CAX). IS: *Inga* species. EC: *Eschweilera coriacea*. PS: *Protium* species. LS: *Licania* species.

Table S3. Turgor loss point (TLP) and bulk leaf osmotic potential (π_o) estimates (mean ± SE) using the methods described by Sack et al. (2011) on PrometheusWiki. Trait values are given for the four species representing one of the four plant functional types characterized in this study for Caxiuanã National Forest (CAX). Data for each species are separated by drought treatment. IS: *Inga* species. EC: *Eschweilera coriacea*. PS: *Protium* species. LS: *Licania* species.

Figure S1. Frequency distribution of turgor loss point (TLP) estimates from a 10000 iteration bootstrap of the change point detection routine. Tapajós (TNF): grey bars. Caxiuanã (CAX): textured bars. (a) *Inga* represents early-successional drought-intolerant. (b) *Eschweilera* represents late-successional drought-intolerant. (c) *Protium* represents early-successional drought-tolerant. (d) *Licania* represents late-successional drought-tolerant.

Figure S2. Pressure-volume curves showing the relationship between leaf water potential (MPa) and leaf water loss (mmol H_2O cm^{-2}) for species from each plant functional type measured in the control and drought plots at Caxiuanã. (a) *Inga*: early-successional drought-intolerant. (b) *Eschweilera*: late-successional drought-intolerant. (c) *Protium*: early-successional drought-tolerant. (d) *Licania*: late-successional drought-tolerant. No significant differences were detected between treatments for any species using the change-point detection routine, but *Inga* was significantly different between treatments using the PrometheusWiki protocol.

Figure S3. Xylem vulnerability curves showing the percent loss in conductance (PLC, %) with decreasing xylem pressure (MPa) for species from each plant functional type measured in the control and drought treatment plots at Caxiuanã. (a) *Inga*: early-successional drought-intolerant.

(b) *Eschweilera*: late-successional drought-intolerant. (c) *Protium*: early-successional drought-tolerant. (d) *Licania*: late-successional drought-tolerant.

Figure S4. Leaf pressure-volume (p-v) curve with the leaf water potential inverted ($1/\Psi$, MPa^{-1}) on the y-axis versus the reduction in relative leaf water content (100-RWC, %). The "linear" portion of each curve is shown by closed black dots, which is determined by the *acceptance criteria* of 5 data points and an $R^2 > 0.90$. (a) Full p-v curve using data from the PrometheusWiki template (Sack *et al*. 2011). (b) The same p-v curve as panel (a), except the y-axis is expanded to reveal the curvature in the "linear" portion. The turgor loss point (*TLP*) and osmotic potential (π_o) estimates from these data are given in the inset. (c) The same p-v curve as panel (b), except the data selected for the "linear" portion are shifted by two to the left. In this scenario, we assume the data points on the right were not measured because the acceptance criteria had been met. *TLP* and π_o increase by 0.49 and 0.38 MPa, respectively. (d) The same p-v curve as panel (b), except one additional, and hypothetical, measurement is added to the curve (denoted by red star) to give a "linear" portion that is shifted to the right by one data point. The new data point was linearly extrapolated from the two adjacent data points. *TLP* and π_o decrease by 0.17 and 0.15 MPa, respectively.

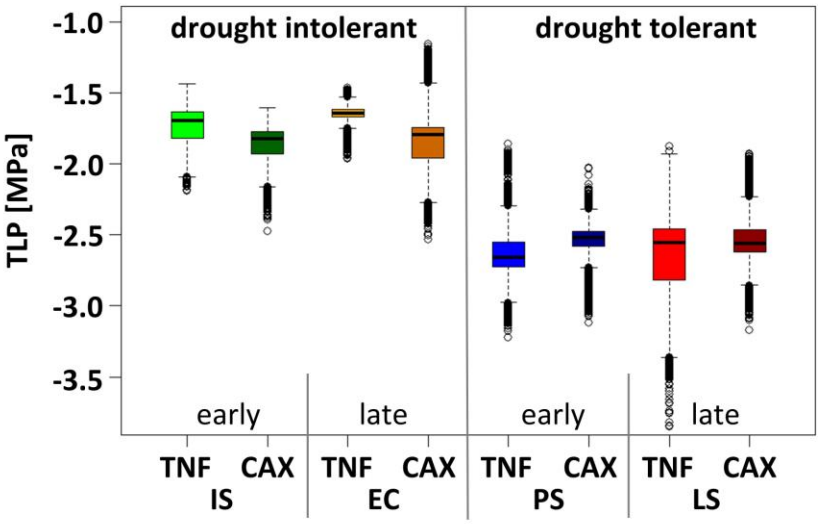

Figure 1.

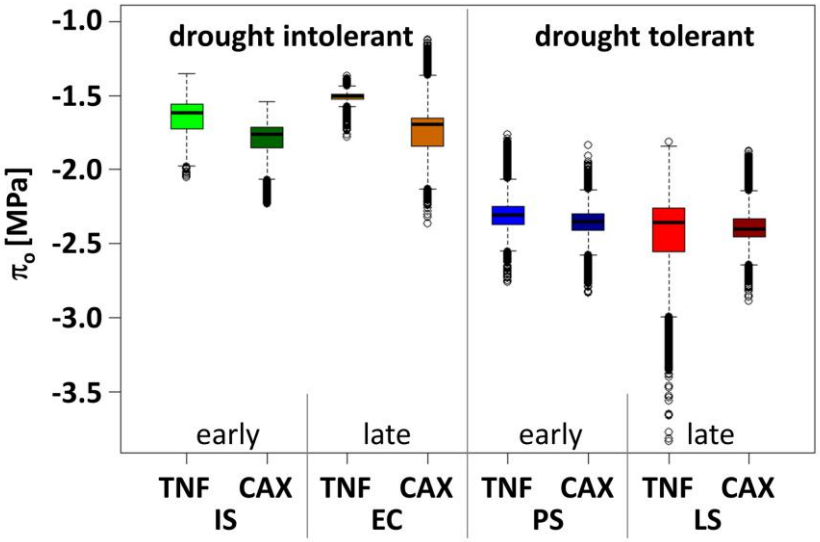

Figure 2.

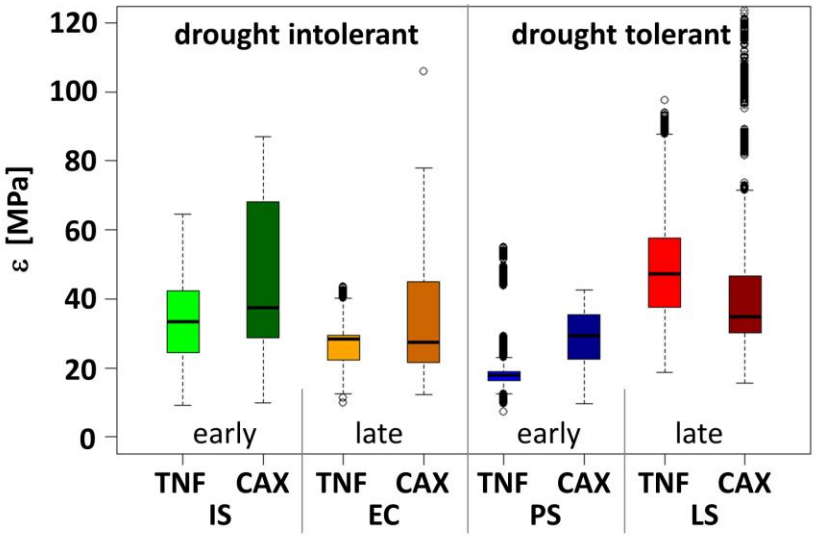

Figure 3.

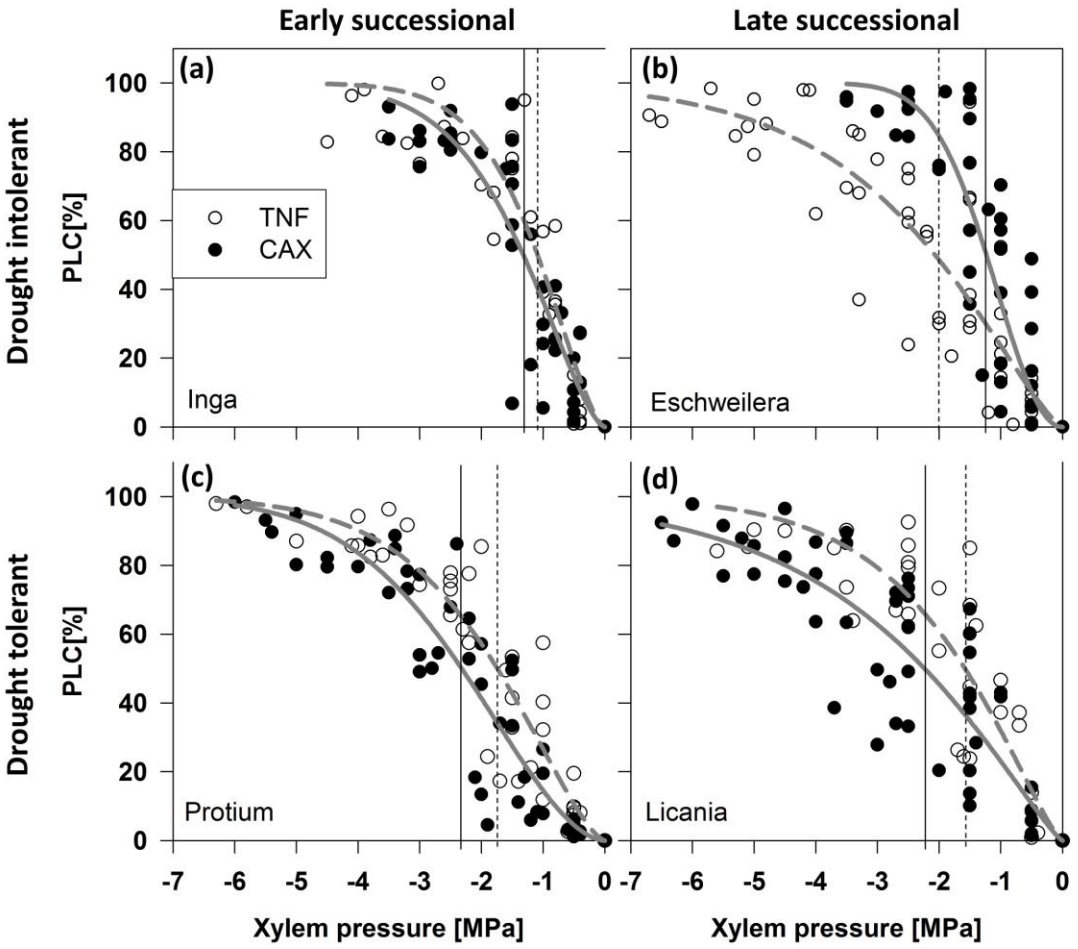

Figure 4.

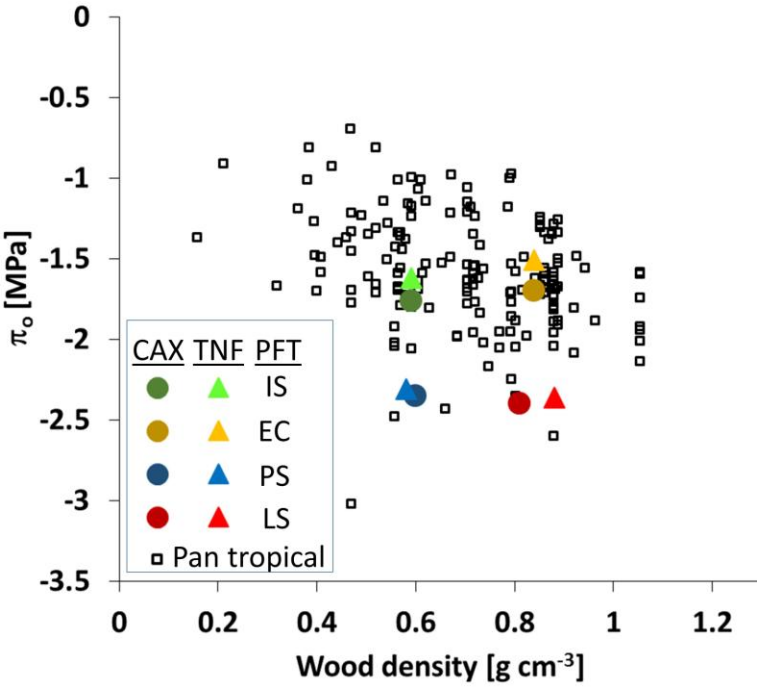

Figure 5.